Contents list available at CBIORE journal website

International Journal of Renewable Energy Development

Journal homepage: https://ijred.cbiore.id

Research Article

A multi-objective metaheuristic framework for reactive power market optimization in distributed renewable systems

Luis M. Sanz[a,b*], Joaquín Pacheco[a], Silvia Casado[a]

[a] *University of Burgos, Department of Applied Economics, Burgos, 09001, Spain*

[b] *MOEVE, Exploration and Production, Madrid, 28046, Spain*

Abstract. The increasing integration of renewable energy sources into the electrical grid demands specific ancillary services, particularly for reactive power supply and voltage control. This study introduces an optimization framework integrated with a reactive power market under a high penetration of distributed generation (DG). The methodology formulates a multi-objective optimization problem with five technical and economic objective functions, solved using a multi-objective metaheuristic algorithm (MOPSO) and selecting the operating point from the Pareto front through TOPSIS. It also integrates a VCG auction mechanism to allocate the reactive power demanded by the system operator, promoting truthful bidding under the usual VCG assumptions. Validation is performed on a modified IEEE-30 test system with 50 MW DG units at buses 19, 21 and 30 and a stressed load condition at the same buses. The TOPSIS selected operating point under scenario S3 achieves active power losses of 2.382 MW, voltage deviation of 0.194 p.u., and conventional generation cost of 7648 \$, while the S3 Pareto front reaches a hypervolume of 0.823. In the reactive power auction based on 20.2 MVAr demand, VCG allocates 100 % of the procurement to renewable units for total payments of 60.71 \$. The results confirm that the proposed model significantly improves the technical operation of the system while providing an economically viable framework for the integration of reactive power ancillary services into electricity distribution, supporting the transition towards more efficient, stable and sustainable electrical networks.

Keywords: Distributed generation, MOPSO, multi-objective optimization, reactive power market, renewable energy sources, VCG auction

Received: 25th Dec 2025; Revised: 18th May 2026; Accepted: 5th July 2026; Available online: 17th July 2026

1. Introduction

The new energy transition, driven by decarbonization policies and the proliferation of distributed renewable energy sources (RES), is transforming the topology and operation of electrical grids (Blaabjerg *et al.,* 2017). Reactive power plays a fundamental role in the operation of a power system, ensuring security and efficiency while reducing transmission and distribution losses (Mugemanyi *et al.*, 2020). Distributed generation (DG) plants, mainly photovoltaic and wind plants equipped with power electronic converters, offer unique capabilities for the control of reactive power in real time. This characteristic makes them key players in providing ancillary voltage control and stability services to the grid (Iweh *et al.*, 2021). Therefore, in existing electrical assets characterized by the growing integration of DG, ancillary services are gaining unprecedented importance (Molzahn *et al.*, 2017).

However, most electrical system operators do not have adequate market mechanisms to encourage the participation of DG in the voltage control service. Traditionally, reactive power needs have been scheduled and purchased by transmission system operators (TSOs) from large generating plants through mandatory requirements or fixed remuneration (Singh *et al.*, 2011).

The lack of economic incentives for DG plants to participate in ancillary voltage control services constitutes a significant barrier to network optimization. In many countries, these facilities are required to supply reactive power at zero cost or, in the case of smaller plants, are not required to participate (Acosta *et al.*, 2021). This situation wastes a valuable resource for the grid and can lead renewable plants to unnecessarily oversize their power converters to meet mandatory requirements.

The literature reveals a disconnection between technical optimization and market design. Technical studies reduce losses and improve voltage profiles but provide no economic mechanism to incentivize DG participation in reactive provision. On the other hand, the existing reactive-market proposals either rely on pay-as-bid or bilateral contracts that do not guarantee truthful bidding, or, the reactive procurement size is imposed rather than derived from the actual technical needs of the network. This study addresses this problem by proposing a comprehensive reactive power market model, which is applicable to networks with highly integrated DG, where the amount of reactive power needed is derived from multi-objective optimization and selected through multi-criteria decision-making (TOPSIS). The model uses a Vickrey-Clarke-Groves (VCG) auction mechanism, extensively analyzed in combinatorial auction theory (Cramton *et al.*, 2006), for efficient allocation of reactive power among all suppliers connected to

* Corresponding author
Email: sanziaei@gmail.com (L.M.Sanz)

the same bus, incentivizing disclosure of true costs and maximizing social benefits.

The main contributions of this study are the following:

- An integrated multi-objective optimization–market framework that couples a five-objective MOPSO optimization, balancing active losses, voltage deviation, Fast Voltage Stability Index, conventional generation cost and DG reactive cost, with a market clearing stage. The reactive procurement size is derived from the technical Pareto front rather than externally imposed.
- An adaptation of the Vickrey-Clarke-Groves auction to the physical and economic specifics of reactive power provision, including temporal factors (*Kt*), technology (*Dr*) and capacity reserve (*CPr*) that preserve the incentive compatibility property of standard VCG while accommodating the DG heterogeneity of different technologies. The extended factors are introduced as a possible regulatory layer for future market designs.
- An implementation of a TOPSIS decision-making stage that maps the Pareto front to a single operating point under DSO-defined weights.
- Quantitative analysis of the technical and economic impact of the proposed market on the standard IEEE-30 test system, offering numerical evidence of incentive compatibility in a reactive auction with heterogeneous DG.

The rest of the paper is organized as follows. Section 2 presents a review of the literature on reactive power markets and grid optimization with DG. Section 3 formulates the mathematical optimization model, including objective functions and constraints, the proposed VCG auction mechanism, and details the metaheuristic optimization algorithm used in the model. Section 4 presents the computational and cost allocation results. Finally, Section 5 presents the conclusions of the paper and future research directions.

2. Literature review

Reactive power optimization has been explored in several scientific articles as a fundamental problem in the operation of electrical networks (Liu *et al*., 2021; Wu *et al*., 2010). The optimal power flow problem (OPF) was formulated more than 60 years ago, but even today there is no robust and computationally efficient technique to solve it completely for extensive networks (Prioste, 2021).

From a mathematical point of view, the problem is highly nonlinear, with both equality and inequality constraints, and includes both discrete (e.g., transformer tap regulation) and continuous (e.g., bus voltage) control variables. This complexity has led to the development of a variety of solving approaches, from classical mathematical programming methods to metaheuristic techniques (Bukhsh *et al*., 2013).

In recent years, metaheuristic multi-objective optimization algorithms have been extensively used for their ability to handle this type of complex model, providing acceptable solutions at a reasonable computational cost (Zhang *et al*., 2016). These methods allow multiple objectives, such as loss minimization, improved voltage profile, network stability, and generation cost minimization, to be addressed simultaneously.

The high integration of DG is transforming the operation of electricity grids, mainly at the distribution level. DG based on RES has characteristics that can be both a challenge and an opportunity for voltage control. On the one hand, the intermittency and variability of the RES can cause voltage fluctuations and quality problems. On the other hand, most of these installations use power electronic converters which, if properly controlled, can provide fast and accurate reactive power control (Javed *et al*., 2023). In fact, converters have the ability to inject or absorb reactive power. This capacity depends on the oversizing of the electronic converter and the active power it is injecting into the network. An oversizing of only 10% in the converter can provide a reactive capacity of 46% when operating at full load, while an oversizing of 30% can provide a reactive capacity of 86%.

This flexibility can be very valuable for the Distribution System Operator (DSO) in using the reactive control capability of the DG to improve the voltage profile, reduce losses, and increase the stability of the system. However, appropriate market mechanisms must be developed to incentivize the participation of these sources in the ancillary voltage control service (Safari *et al*., 2020).

Reactive power markets have some characteristics that differentiate them from markets for active power. Reactive power is not easily transportable over long distances as a result of the associated high losses, therefore, it must be generated close to the final consumer. This local characteristic means that reactive markets are likely to be less competitive and more susceptible to monopoly problems.

Several approaches have been proposed to develop reactive power markets, each addressing different operational and economic aspects. Traditional methods, such as fixed remuneration schemes and mandatory procurement by TSOs, have shown limitations in incentivizing DG participation. More recent proposals include: zonal markets reflecting the local characteristic of reactive power (Wolgast *et al*., 2022), auction mechanisms for the competitive procurement of reactive power ancillary services (Tesfatsion, 2020), remuneration based on the availability and use of reactive power (Halbhavi *et al*., 2012), and long-term capacity contracts and spot markets for short-term needs.

The practical implementation of reactive power markets remains limited. According to Häselbarth *et al*. (2023), reactive markets in Germany have the potential to turn over EUR 1.1 billion annually by 2035, and could exceed EUR 2 billion by 2050. However, the current situation is that the market for reactive power supply is at a high voltage level, based on long-term contracts between TSOs and some generating companies. Challenges such as standardizing market participation rules, ensuring fair competition, and integrating DG into existing market structures persist.

Reactive power management has been explored in recent years, showing a lack of connection between technical optimization and the design of market mechanisms. Technical optimization studies have achieved notable results: Xu *et al*. (2022) successfully demonstrated multi-objective evolutionary algorithms for electrical networks, while Mohammed *et al*. (2024) reported important power loss reductions through advanced planning methods. However, these technically focused studies present a lack of economic incentive mechanisms for DG participation in reactive power provision. Li and Xiong (2024) optimize power losses and voltage deviation in distribution networks with high DG integration. Although their approach demonstrates strong technical optimization capabilities, it provides no market clearing mechanisms and fails to establish incentive structures for DG participation. Similarly, Candra *et al*. (2024) propose optimal allocation of reactive resources in distribution grids, but their work does not develop a market framework and lacks integration of multi-objective optimization with VCG mechanisms. Qiu *et al*. (2024) developed sophisticated bi-level optimization frameworks for ancillary service markets with a study focused on active power and frequency services rather than reactive power support.

From a market design perspective, Liu *et al.* (2024) develop a stochastic electricity market that incorporates VCG mechanisms for handling uncertainties. Although their VCG design is robust, the study does not address reactive power or connections with technical optimization. Bozionek *et al.* (2022) propose a multi-level market design that enables DG to provide reactive power services at distribution-transmission levels. While this hierarchical market architecture is innovative, it does not integrate multi-objective optimization techniques or implement VCG clearing mechanisms. Malik *et al.* (2023) successfully implemented market mechanisms that maximize energy trading volumes while ensuring truthful bidding, particularly during off-peak periods. Potter *et al.* (2023) propose a reactive power market at the distribution level specifically designed for the participation of DG. Despite considering DG integration, their approach neither employs VCG mechanisms nor utilizes multi-objective technical optimization for demand determination. Siahroodi *et al.* (2022) introduce an innovative concept using electric vehicles within a stochastic multi-objective reactive market framework. However, in the study, there is no adapted VCG auction mechanism, TOPSIS decision-making integration, or market structuring. Finally, Anaya and Pollitt (2020) provides a comprehensive review of international procurement practices for reactive power and associated regulatory approaches. This work is purely a regulatory and economic review without proposing optimization algorithms or VCG clearing mechanisms.

The present work addresses an integrated framework that combines: multi-objective optimization using MOPSO for determining non-dominated solutions of five technical and economic objectives, decision-making for selecting optimal solutions belonging to the obtained Pareto front, and VCG-based market clearing mechanisms ensuring incentive compatibility. The proposed model is tested on a modified IEEE-30 test network. From the optimization perspective, this meshed network is computationally more challenging, since power flows can be distributed across multiple paths, resulting in a larger number of control variables, nonlinear constraints, and potential non-convexities in the solution space.

3. Materials and methods

The reactive power optimization problem in electrical networks with DG is formulated as a multi-objective optimization problem and solved through two stages: first, a Pareto-based metaheuristic optimization algorithm (MOPSO) to generate the set of non-dominated operating points, and second, multi-criteria decision-making (TOPSIS) to select a compromise solution from which the reactive power requirements are derived and submitted to the reactive market for VCG-based clearing.

It is important to clarify that the five objective functions are not aggregated into a single weighted function. The optimization is performed in the original five-dimensional objective space using Pareto dominance. MOPSO therefore returns a set of non-dominated operating points, not a single solution, and no weighting factor is applied during the optimization stage. Weighting is introduced in the TOPSIS decision-making stage to select a single compromise operating point.

3.1 Mathematical formulation of the multi-objective problem

Without loss of generality, this problem can be represented as: $minF = [f_1, f_2, \dots, f_5]$, subject to inequality constraints $h_k \leq 0$ for $k=1,2,\dots,H$ and equality constraints $g_j=0$ for $j=1,2,\dots,G$, where f_i represents each goal to be minimized.

We define the vector of control variables as: $u = [V_G, P_G, T_{TX}, Q_C, Q_{DG}, P_{DG}]$ where V_G and P_G represent the output voltage and active power of conventional synchronous generators located on buses 1, 2, 5, 8, 11, 13 in the IEEE-30 test network, T_{TX} indicates the position of transformer tap-changers, Q_C refers to reactive power compensation from existing capacitor banks, P_{DG} and Q_{DG} denote active and reactive power from DG sources. Capacitor banks are considered mandatory assets without remuneration through the proposed reactive power market. Our market design focuses exclusively on the remuneration of reactive power supplied by DG units, as they represent the flexible and incentivized resources in the system. The technical effect of capacitor banks is still captured in optimization, as they influence voltage support, losses, and stability, but they are not part of the economic decision-making process.

3.1.1. Objective functions

Five objectives are considered, equations 1-5: P_{loss} represents the active power losses in the distribution lines; V_{TVD} is the total voltage deviation from the reference value; S_{FVSI} is the network stability index; G_{cost} reflects the generation cost of conventional generators; and C_{QDG} represents the cost associated with the reactive power supplied by RES DG sources.

$$f_1 = P_{loss} = \sum_{i,j \in N_b} G_{ij} \left[V_i^2 + V_j^2 - 2V_iV_j \cos(\theta_i - \theta_j) \right] \quad (1)$$

$$f_2 = V_{TVD} = \sum_{i=1}^{N_b} \left| V_i^{ref} - V_i \right| \quad (2)$$

$$f_3 = S_{FVSI} = \max_{(i,j) \in \mathcal{L}} \left[\frac{4Z_{ij}^2 Q_j}{V_i^2 X_{ij}} \right] \quad (3)$$

$$f_4 = G_{cost} = \sum_{g=1}^{N_G} \left(a_g + b_g P_{G_g} + c_g P_{G_g}^2 \right) \quad (4)$$

$$f_5 = C_{Q_{DG}} = \sum_{t=1}^{t_p} \sum_{r=1}^{N_i^{DG}} \sum_{i=1}^{\mathcal{J}^{DG}} \left[C_{r,t|i}^{Q_{DG}} \quad \left| Q_{r,t|i}^{DG} \right| \right] \approx Q_{req} \quad (5)$$

In f_1 (Eladl *et al.*, 2022), G_{ij} is the conductance between buses i and j, V_i and V_j are the bus voltages, and θ_i and θ_j are the phase angles. In f_2 (Bamikole *et al.*, 2024), N_b is the total number of buses, V_i^{ref} is the reference voltage (typically 1.0 p.u.), and V_i is the voltage on bus i obtained from the execution of power flow. In f_3 (Musirin and Rahman, 2002), Z_{ij} and X_{ij} are the line impedance and reactance between the nodes i and j, Q_j is the reactive power at the destination node and L is the set of distribution lines. In f_4 (Wood *et al.*, 2013), a_g, b_g, and c_g are cost coefficients for generator g, N_G is the number of conventional generators and P_{Gg} is the active power generated by each unit. f_5 is the cost associated with reactive power supplied by renewable sources (Gandhi 2020), where t_p is the evaluation period, N_i^{DG} is the number of DG plants connected to bus i, $\mathcal{J}^{DG}$ is the set of buses with DG, $C_{r,t|i}^{Q_{DG}}$ is the cost associated with reactive generation from plant r connected to bus i in period t, and $Q_{r,t|i}^{DG}$ is the reactive power generated or absorbed.

The selection of our five-objectives balances the technical and economic requirements that must be addressed in modern electrical networks. f_1 (active power losses) remains fundamental to any power system optimization and directly affects the operational efficiency of the DSO. f_2 (total voltage deviation) is required to comply with regulatory standards, directly affecting power quality. f_3 (fast voltage stability index) is critical for N-1 security assessment. It provides a simple, yet effective measure of proximity to voltage instability, and it can be computed directly from load flow results without the need for computationally intensive eigenvalue analysis. FVSI requires only local measurements without a full Jacobian calculation. This simplicity is critical in multi-objective metaheuristic algorithms, where thousands of evaluations are required (Sachan *et al.*, 2025). f_4 (generation cost) ensures that conventional generation costs remain minimal while maintaining network quality and security. f_5 (DG reactive provision) incentivizes DG units to participate in reactive markets with the minimum cost to the DSO.

3.1.2. Equality and inequality constraints

The problem is subject to various technical and operational constraints. The fundamental constraints on power balance for any electrical network are expressed through the AC power flow equations 6 and 7, which ensure the balance between generation and demand. The characteristics of these equations differ significantly between transmission and distribution networks. Transmission networks have a low R/X ratio, which means small angle differences and valid decoupled approximations. Distribution networks, on the other hand, have a higher R/X ratio and strong coupling between active and reactive flows. In our study, we have used the full set of AC power flow equations without simplifications.

$$\sum_{g=1}^{N_G} P_{G_g} - \sum_{l=1}^{N_L} P_{L_l} + \sum_{r=1}^{N_{DG}} P_r^{DG} = V_i \sum_{i,j=0}^{N_b} V_j \left(G_{ij}\cos\theta_{ij} + B_{ij}\sin\theta_{ij}\right) \quad (6)$$

$$\sum_{g=1}^{N_G} Q_{G_g} + \sum_{c=1}^{N_C} Q_{C_c} - \sum_{l=1}^{N_L} Q_{L_l} + \sum_{r=1}^{N_{DG}} Q_r^{DG} = V_i \sum_{i,j=0}^{N_b} V_j \left(G_{ij}\sin\theta_{ij} - B_{ij}\cos\theta_{ij}\right) \quad (7)$$

where: P_{G_g}, P_{L_l} and P_r^{DG} are the active power of the generator g, the active power demand at load l, and the active power from the DG source r. Q_{G_g}, Q_{C_c}, Q_{L_l} and Q_r^{DG} are the reactive power of the generator g, the reactive power of the capacitor bank c, the demand for reactive power at load l, and the reactive power of the DG source r. B_{ij} is the susceptance between buses i and j. θ_{ij} is the angle difference between the buses i and j.

In addition, generator operating limits, bus voltage limits, capacitor bank limits, transformer tap-changer, and DG sizing limits are the main inequality constraint of the model.

$$P_{G_g}^{min} < P_{G_g} < P_{G_g}^{max}, \quad g = 1,2,\dots,N_G \quad (8)$$
$$Q_{G_g}^{min} < Q_{G_g} < Q_{G_g}^{max}, \quad g = 1,2,\dots,N_G \quad (9)$$
$$V_{G_g}^{min} < V_{G_g} < V_{G_g}^{max}, \quad g = 1,2,\dots,N_G \quad (10)$$
$$V_i^{min} < V_i < V_i^{max}, \quad i = 1,2,\dots,N_b \quad (11)$$
$$Q_{C_c}^{min} < Q_{C_c} < Q_{C_c}^{max}, \quad c = 1,2,\dots,N_C \quad (12)$$
$$\tau_q^{min} < \tau_q < \tau_q^{max}, \quad q = 1,2,\dots,N_{TX} \quad (13)$$
$$S_{L_l} \le S_{L_l}^{max}, \quad l = 1,2,\dots,N_L \quad (14)$$
$$P_{r,min}^{DG} < P_r^{DG} < P_{r,max}^{DG}, \quad r = 1,2,\dots,N_{DG} \quad (15)$$
$$Q_{r,min}^{DG} < Q_r^{DG} < Q_{r,max}^{DG}, r = 1,2,\dots,N_{DG} \quad (16)$$

$$|Q_r^{DG}| \le \sqrt{\left(S_{r,max}^{DG}\right)^2 - (P_r^{DG})^2} \quad (17)$$

where $P_{G_g}^{min}$ and $P_{G_g}^{max}$ represent the minimum and maximum active power limits for each conventional generator g, while $Q_{G_g}^{min}$ and $Q_{G_g}^{max}$ define the reactive power limits for these same generators. The output voltage of each generator is bounded between $V_{G_g}^{min}$ and $V_{G_g}^{max}$, and similarly, the voltage at each bus i in the system must be maintained between V_i^{min} and V_i^{max}. The capacitor banks, modeled by Q_{C_c} (with $c = 1,2,\dots,N_C$), have operational restrictions between $Q_{C_c}^{min}$ and $Q_{C_c}^{max}$. The setting of the tap-changer of the transformers τ_q (where $q = 1,2,\dots,N_{TX}$) varies within the range $\left[\tau_q^{min}, \tau_q^{max}\right]$. The capacity of the distribution line is limited by $S_{L_l} \le S_{L_l}^{max}$ for each line l (out of a total of N_L lines). For DG units, $P_{r,min}^{DG}$ and $P_{r,max}^{DG}$ delimit the injection of active power by each unit r (out of a total of N_{DG} units), while $Q_{r,min}^{DG}$ and $Q_{r,max}^{DG}$ establish the limits of the reactive power. Finally, equation 17 models the converter capacity constraint, where $S_{r,max}^{DG}$ is the maximum apparent power of the DG unit r, P_r^{DG} and Q_r^{DG} are the active and reactive power output of unit r. Equation 17 assumes that the distortion power component due to harmonics is negligible compared to the fundamental frequency components. In real distribution networks with high penetration of converter-based DG and nonlinear loads, harmonic distortion can affect the apparent power and voltage profiles.

3.2. Multi-objective optimization and decision-making algorithms

The MOPSO metaheuristic algorithm has been selected to implement our optimization problem. In the area of multi-objective optimization, MOPSO is one of the main algorithms that have been used in several fields of optimization (Nkalo *et al.*, 2024). The Multi-Objective Particle Swarm Optimization approach was presented by Coello *et al.* (2004), and addresses the application of particle swarm optimization to multi-objective problems through the implementation of Pareto fronts. The algorithm is able to maintain a diverse set of solutions and converge to the true Pareto front. The main principle is the use of an external archive to store the best non-dominated solutions found by each particle throughout the iterations, combining the convergence power of PSO with Pareto dominance concepts. The algorithm uses adaptive hypercubes for diversity preservation and a roulette-wheel selection mechanism. This algorithm is easy to implement, has few parameters to adjust, and does not require gradient information during the optimization process.

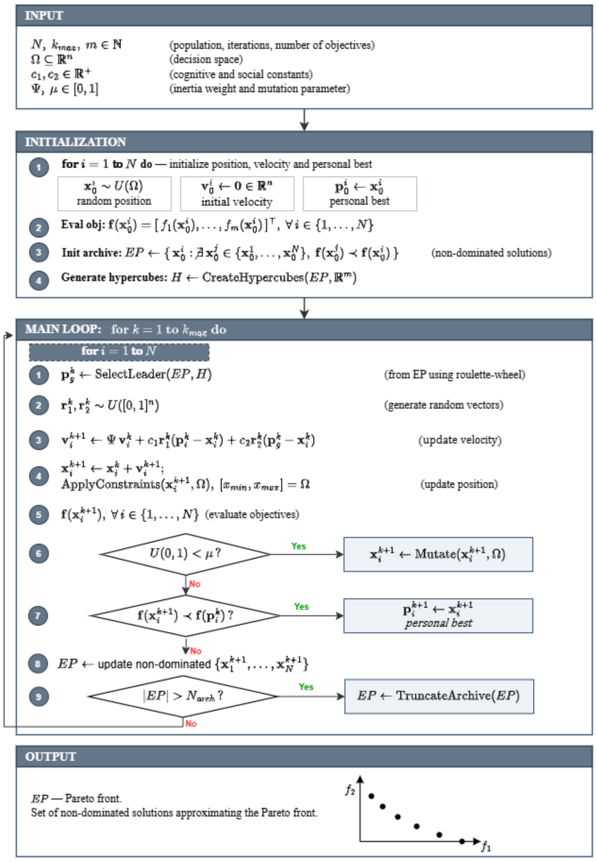
Fig. 1. Multi-Objective Particle Swarm Optimization (MOPSO) algorithm.

The MOPSO algorithm is mainly composed of the following stages: initialization of the population, initial evaluation of the objectives, Pareto front identification, adaptive hypercube generation, leader selection, velocity and position update, mutation operator application, and external archive management. The objective space is divided into hypercubes, which are regions with as many dimensions as objectives to minimize. The number of regions is defined by the user before starting the optimization. The initial inertia weight and damping factor, which control the transition from global to local search, are set to 0.9, while the cognitive and social coefficients, which govern particle attraction to personal and global best positions, are set to 2. A grid-based archive with 15 subdivisions per dimension manages non-dominated solutions. The mutation coefficient is set to 0.5, and the external archive size and leader selection pressure are set to 500 and 2, respectively. Figure 1 shows a simplified pseudocode of the MOPSO algorithm.

3.2.1. TOPSIS decision-making and weighting strategies

After having a set of non-dominated solutions, we need to decide which optimal solution is going to be implemented in the test network. To accomplish that, we use TOPSIS - Technique for Order Preference by Similarity to the Ideal Solution (Chen and Hwang, 1992), which is a Multi-Criteria Decision-Making (MCDM) technique based on the measurement of the distance of the optimal solutions with respect to an ideal point and its opposite. This method has been used successfully in various disciplines such as human resources management, engineering, water management, etc. (Behzadian *et al.*, 2012). As indicated by Huang and Li (2012), TOPSIS has numerous advantages as a decision-making method such as good and well-balanced solutions obtained, the method is similar to rational decision-making, it obtains the best and worst solution simultaneously, and it has good computational efficiency, which makes it suitable for real-time implementations.

3.3. Design of the Reactive Power Market

The reactive power market proposed in this work is specifically designed for electrical networks with a high penetration of DG. Unlike traditional ancillary markets for reactive power, the proposed model recognizes the critical role that DG based on RES can play in the ancillary voltage control service.
The reactive power market model is based on the following fundamental principles:

- Divide the network considering loss optimization criteria and reactive power localization.
- Establish clear and transparent rules for the participation of all DG plants.
- Promote competition to avoid monopoly or oligopoly situations.
- Ensure economic efficiency through the minimization of total costs for the DSO while ensuring fair remuneration for suppliers.
- Ensure that the solutions obtained comply with the technical requirements of the DSO/TSO.

The market is structured around the following elements:

- Participants in the reactive market are the DSO as the sole buyer and the DG plants (mainly RES) equipped with power converters capable of controlling reactive power or small conventional generation plants.
- The product is a reactive power contract (*CR*) defined by three main components:

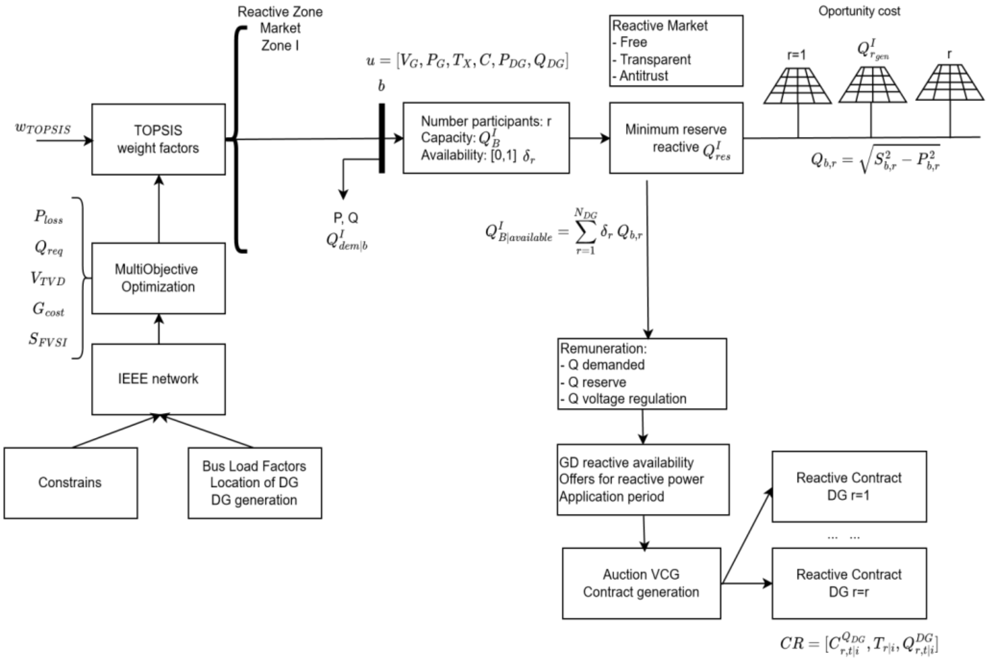

Fig. 2. Hierarchical framework for reactive power market implementation with integrated TOPSIS-based multi-objective optimization methodology.

$$CR = \left[C_{r,t|i}^{Q_{DG}}, T_{r|i}, Q_{r,t|i}^{DG}\right] \quad (18)$$

where $C_{r,t|i}^{Q_{DG}}$ is the price bid of DG plant r connected at bus i, $T_{r|i}$ is the application period and $Q_{r,t|i}^{DG}$ is the reactive capacity bid.

- The market is divided into hourly periods ($T = 1h$), with the possibility of longer-term contracts.
- A Vickrey-Clarke-Groves (VCG) auction is used for each bus and period.

The operation of the proposed market follows the following steps: the DSO determines the reactive power requirements ($Q_{req|i}^{I}$) for each bus and zone, following the multi-objective optimization process; next step is the auction announcement where the DSO publishes the reactive power requirements for each bus and period; DG plants interested will submit their bids for reactive power and the bid price, $Q_{r,t|i}^{DG}$ and $C_{r,t|i}^{Q_{DG}}$; auction using VCG algorithm determines the winners and the prices to be remunerated and a contract is issued between the stakeholders during the specified period where suppliers deliver reactive power contracted, and the DSO makes payments accordingly.

Since reactive power cannot be transported efficiently over long distances, the market shall be applied to network zones where local reactive power supply and demand can be balanced. Several methodologies have been proposed in the literature for defining reactive power market zones. Impedance-based electrical distance methods utilize the bus impedance matrix to determine zone boundaries (Ruan *et al.*, 2020). Another method is the use of voltage reactive sensitivity analysis where buses that have a similar voltage magnitude behavior to reactive power injections are clustered (Ji *et al.*, 2023). Clustering approaches such as k-means (Miraftabzadeh *et al.*, 2023) or hierarchical clustering (Zhang *et al.*, 2020) applied to load flow or sensitivity indices are additional approaches that can be used. Spectral clustering algorithms have emerged as the predominant technical approach for zone partitioning, where the zoning problem is transformed into graph segmentation, representing power systems as weighted graphs (Hasanvand *et al.*, 2025). In our study, the IEEE-30 test network was used mainly for proof of concept and, given its relatively small size, we considered it as a single zone. This simplification allows us to focus on validating the integration of multi-objective optimization with the VCG auction market design.

3.3.1. VCG auction mechanism for reactive power

The VCG auction mechanism is used to determine which suppliers will provide the necessary reactive power and what price they will receive. The VCG mechanism has desirable properties, such as incentives for true bids and economic efficiency. The VCG auction mechanism used for reactive power markets includes multi-factor adjustments in order to provide the flexibility needed for DG sources. While preserving the incentive compatibility properties of standard VCG, our adaptation addresses the physical and economic characteristics unique to reactive power provision from DG sources. The payment structure can be seen in equation 19. For each DG source r, the VCG_m payment is calculated as:

$$VCG_m(r) = VCG(r) \cdot K_t \cdot D_r + CP_r \quad (19)$$

$$VCG(r) = C_{TOT}\left(N_{r|i}^{DG} \setminus \{r\}\right) - \left[C_{TOT}\left(N_{r|i}^{DG}\right) - C_{offer}(r)\right] \quad (20)$$

where: $N_{r|i}^{DG}$ is the set of market participants for the bus i. $C_{TOT}\left(N_{r|i}^{DG} \setminus \{r\}\right)$ is the total cost without the participation of the supplier r. $C_{TOT}\left(N_{r|i}^{DG}\right)$ is the total cost with all participants, and $C_{offer}(r)$ is the supplier's offer. The objective of the algorithm is to minimize the total cost to the DSO, $min\ C_{TOT}\left(N_{r|i}^{DG}\right)$, subject to the reactive needs identified in the multi-objective optimization process. $VCG(r)$ represents the base VCG payment calculated using equation 20. The adaptation introduces three key adjustments. The temporal factor K_t differentiates payments between time periods, reflecting that reactive power support has a higher value during peak demand when voltage regulation is critical. The technology factor D_r recognizes the operational differences between the DG sources, such as battery storage, solar or wind technology. The capacity payment CP_r encourages the maintenance of reactive reserves for system security.

In our model, all factors have been set to unity ($K_t = D_r = 1$) and CP_r defaults to zero, reducing the mechanism to standard VCG. This adaptation allows DSOs to begin with a simple implementation equivalent to standard VCG and progressively introduce sophistication as the market matures and operational experience is accumulated. The default configuration establishes a baseline of performance, demonstrating that even the standard VCG applied within our framework provides significant technical and economic benefits. VCG provides an incentive to the suppliers to show the real cost for providing reactive power because if they bid above their true cost, they increase the risk of not being selected, and if they bid below their actual cost, they increase the risk of being selected at a price that does not cover their costs.

Figure 2 shows the optimization framework and reactive market proposal, where δ_r is a discrete parameter which represents the availability factor for reactive power. This accounts for maintenance schedules (planned unavailability), forced shutdowns (unplanned unavailability) or DG availability in general. The full methodology integrates multi-objective optimization, multi-criteria decision-making and market clearing, into a single workflow. For each market period, the DSO:

- Runs MOPSO over the five-objective formulation to generate the Pareto front of non-dominated operating points.
- Applies TOPSIS with the selected weight vector to obtain the recommended operating point and the resulting bus-level reactive power requirements.
- Publishes the requirements as an auction announcement to all DG units connected within the corresponding bus.
- Receives bids from the participating DG units.

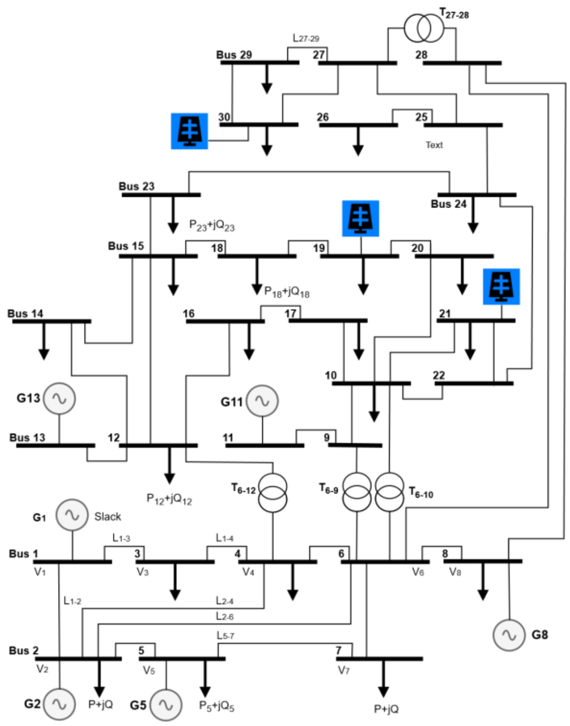

Fig. 3. Single-line diagram of modified IEEE 30 test system with DG integration at buses 19, 21 and 30.

- Clears the auction via the VCG mechanism, determining selected suppliers, allocated reactive power and payments.

DG units are often operated under predefined power factor setpoints according to grid codes, which implies that some reactive power may already be injected or absorbed prior to market participation. In this study, we considered the full reactive power capability of DG units (within their technical Q_{min}, Q_{max} limits) as available for optimization and market allocation, without modeling a fixed initial power factor setpoint. This assumption was made to focus on the design of the market mechanism and the evaluation of multi-objective optimization.
The integration of DG into the design of the reactive power market is challenging due to several factors. First, reactive power is a highly localized service that must be supplied close to the final demand because the reactive power cannot be transmitted over long distances efficiently. Second, the available reactive capacity of the DG units depends on their active power output and converter size, which introduces uncertainty and additional technical constraints. Third, providing reactive power may imply an opportunity cost for DG operators because the allocation for reactive power may reduce the active power injected into the grid. Finally, in zones with few DG units, the risk of a monopolistic market arises requiring auction mechanisms that ensure truthful bidding and economic efficiency, such as the proposed VCG. These aspects make the integration of DG into reactive power markets a complex but essential step to achieve efficiency for future electrical networks.

4. Results and Discussion

4.1. Test system and simulation setup

The proposed framework was implemented in MATLAB using MATPOWER (Zimmerman *et al.*, 2010) to solve the power flow calculations. The IEEE-30 test network has been modified in order to include DG at buses 19, 21 and 30, each rated at 50 MW with full four-quadrant power operation (see Figure 3). To evaluate the reactive power support capabilities of DG units under stressed network conditions, the load demand at those buses has been doubled from their baseline values, which drives the most distant buses close to the lower voltage limit of 0.9 p.u.

The MOPSO multi-objective metaheuristic algorithm is used to search for optimal Pareto solutions, under an optimization problem of five objectives. Each simulation used a population of 200 individuals and 300 iterations. Three independent runs were executed and their best solutions were merged into a common Pareto front.

Five operational scenarios were analyzed to evaluate different control strategies.

- S1. The algorithm optimizes only conventional control variables (transformer and capacitor taps, conventional generator voltage and active power).
- S2. DG reactive power injection/absorption is activated to maintain bus voltages near 1.0 p.u. while minimizing the remaining objectives.
- S3. Combined active and reactive DG control.
- S4. Nominal DG active power injection with reactive power support.
- S5. Nominal DG active power injection without reactive power support.

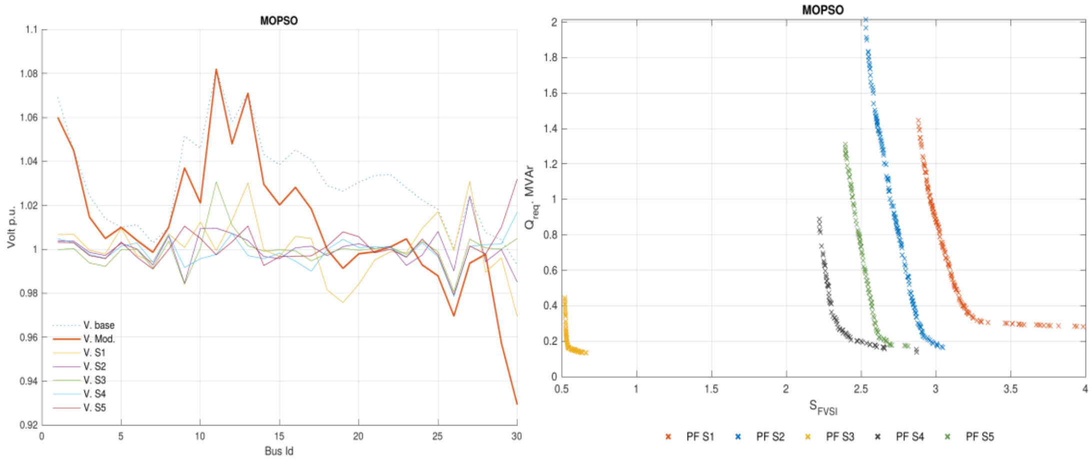

Fig. 4: Voltage profile for the IEEE-30 network. V.base: original network baseline; V.Mod: stressed network (load increase at buses 19, 21, 30 by a factor of two) without DG support; V.S1-S5: stressed network with different optimization scenarios (left); Pareto-fronts for bi-objective optimization, comparing power losses versus total voltage deviation, for all different scenarios (S1-S5) (right).

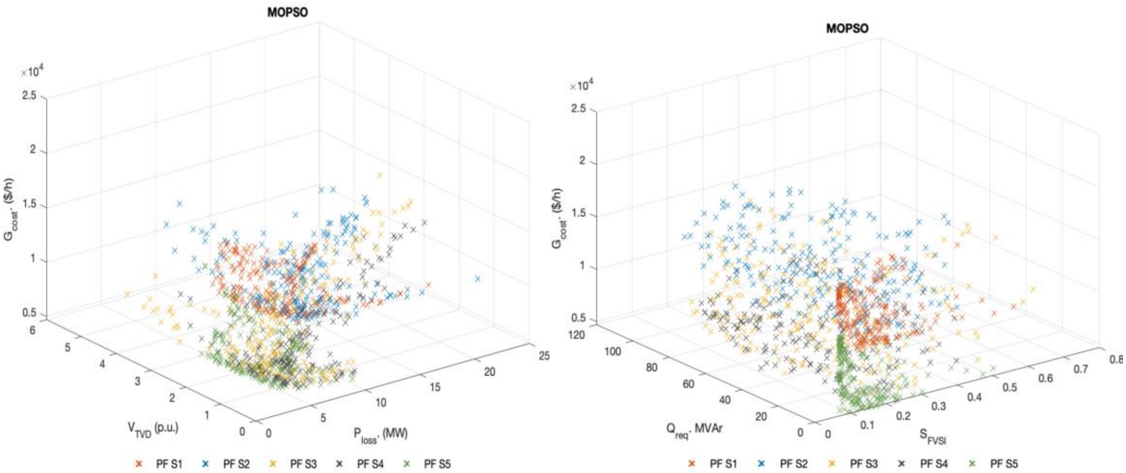

Fig. 5: Pareto fronts for penta-objective optimization. 3D visualization of the fiveobjective optimization space, showing three key objectives: power losses, voltage deviation, and generation cost (left) and power losses, stability index and reactive requirements (right). Each scenario demonstrates progressive improvement in the Pareto fronts.

4.2. Voltage profile and scenario analysis

Figure 4 (left) displays the bus voltages in our IEEE-30 model. *V.Base* represents the voltage profile of the standard IEEE-30 test system under original loading conditions without any modifications or DG integration. *V.Mod* shows the voltage profile under stressed conditions (load doubled at buses 19, 21, 30) without DG support, which constitutes our baseline for comparison. We can observe how the increase in consumption reduces the voltage of some buses close to the limit of 0.9 *p.u.*

The benefits of metaheuristic optimization are clear even in Scenario S1, where only conventional control variables (transformer, capacitor taps and generator settings) are optimized. However, the most distant buses cannot reach the 1.0 p.u. reference value due to the increased load and the associated voltage drop. The use of DG reactive power generation capacity (S2) provides the necessary reactive support to enhance voltage profiles, reducing the voltage deviation of all buses. Scenario S3 mainly reduces power losses through active power injection. Both reactive power injection/absorption and active power injection therefore show clear and complementary effects: reactive support keeps bus voltages around the 1.0 p.u. reference value, while active injection raises local voltages and, due to the proximity of DG to the final load, reduces network losses. Scenarios S4 and S5 are identical, but S5 does not include reactive power support from our DG, and we can see how the power losses increase.

4.3. Pareto front analysis and convergence metrics

Figure 4 (right) shows the bi-objective Pareto fronts (power losses vs. total voltage deviation) for the five scenarios, and Figure 5 presents the penta-objective fronts in two representative 3D projections. The fronts show a progressive improvement from S1 to the DG-enabled scenarios.

Table 1 shows the statistical and convergence metrics obtained by the optimization process under the five-objectives case. *Mean* represents the average value, *Min* and *Max* indicate the best and worst solution values, and *Std D* shows the standard deviation of Pareto solutions. The notation DG *BF* = 2 indicates

Table 1
Statistical performance metrics and convergence indicators of Pareto-optimal solution sets across operational scenarios. Buses with DG = [19,21,30], BF = 2.

		MOPSO BF= 2				
	Obj	S1	S2	S3	S4	S5
Mean	P_{loss}	6.165	6.193	1.396	6.703	3.864
Min		3.736	3.765	0.921	3.112	3.062
Max		13.599	12.384	4.310	17.128	7.265
Std D		1.686	1.691	0.546	3.086	0.598
Mean	V_{TVD}	0.573	0.460	0.190	0.922	0.358
Min		0.442	0.269	0.146	0.264	0.234
Max		0.874	1.441	0.455	5.080	0.941
Std D		0.068	0.127	0.030	0.692	0.097
Mean	G_{cost}	11109.1	11138.8	8182.6	8668.5	6043.6
Min		10487.4	10503.8	7013.5	4774.0	5207.5
Max		12201.8	12017.3	9415.1	17247.2	6601.4
Std D		308.1	335.5	248.1	3383.9	263.0
Mean	S_{FVSI}	0.135	0.095	0.086	0.218	0.112
Min		0.099	0.055	0.069	0.079	0.089
Max		0.221	0.263	0.150	0.509	0.212
Std D		0.017	0.023	0.010	0.085	0.019
Mean	Q_{req}	0.000	14.585	6.220	40.900	0.000
Min		0.000	2.882	0.700	1.660	0.000
Max		0.000	44.389	34.947	104.343	0.000
Std D		0.000	6.758	4.832	26.189	0.000
Hypervolume	PF	0.485	0.512	0.823	0.744	0.804
Avg distance	PF	0.403	0.460	0.303	0.650	0.366
Diversity	PF	0.043	0.069	0.037	0.129	0.060
Spacing	PF	0.028	0.040	0.040	0.044	0.042
Num Sol	PF	475	247	310	200	138

the bus factor, applied to buses 19, 21, and 30 where the DG units are connected. This double load creates voltage stress conditions that demonstrate the critical role of reactive DG power support. The main metrics used to compare the Pareto front are hypervolume, average distance between solutions, diversity index, and spacing. Hypervolume measures the volume of the target space dominated by the solutions. Higher hypervolume indicates better convergence and diversity. The average distance between solutions calculates the average Euclidean distance between each solution in the Pareto front. A lower distance shows that the solutions are grouped in some areas and therefore have less diversity. The diversity index quantifies the spread and distribution of solutions; therefore, a higher index means more diverse solutions. Spacing gives us a metric about the uniformity of the distance between neighboring solutions.

Scenario S3 achieves the lowest mean power losses (1.396 MW) and the lowest mean stability index (0.086), together with a high hypervolume (0.823), indicating both good convergence and competitive front quality. No single scenario dominates across all objectives, confirming the genuinely multi-objective nature of the problem.

4.4. Selection of the operating point via TOPSIS

Table 2 provides the objective values of the operating points selected by TOPSIS under the two weighting strategies. Depending on the TOPSIS weight vector, we can control the electrical network under different quality indicators. Scenario

Table 2
Optimal solutions obtained after multi-objective and TOPSIS optimization for two different strategies w_1 = [0.2,0.1,0.2,0.3,0.2], w_2 = [0.4,0.3,0.2,0.05,0.05].

S	N_{obj}	w_{TOPSIS}	P_{loss}	V_{TVD}	G_{cost}	S_{FVSI}	Q_{req}
S1	5	*w.1*	6.405	0.491	10983.3	0.145	0.000
S2	5	*w.1*	5.131	0.368	11312.2	0.101	14.747
S3	5	*w.1*	1.038	0.155	8288.5	0.079	10.432
S4	5	*w.1*	3.165	0.229	6181.7	0.082	10.236
S5	5	*w.1*	3.821	0.291	6033.0	0.112	0.000
S1	5	*w.2*	8.851	0.588	10685.3	0.113	0.000
S2	5	*w.2*	8.165	0.641	10702.3	0.075	11.357
S3	5	*w.2*	2.382	0.194	7648.8	0.088	2.784
S4	5	*w.2*	3.665	0.330	5867.6	0.090	5.210
S5	5	*w.2*	4.560	0.501	5639.3	0.101	0.000

Table 3
Single-objective optima, extreme points of S4 Pareto front.

Optimization target	P_{loss} (MW)	V_{TVD} (p.u.)	G_{cost} ($)	S_{FVSI} (--)	Q_{req} (MVAr)
min P_{loss}	**2.685**	0.383	6765.8	0.083	16.873
min V_{TVD}	4.032	**0.216**	6696.0	0.217	5.569
min G_{cost}	5.952	0.315	**5293.2**	0.085	16.271
min S_{FVSI}	2.728	0.370	6316.2	**0.067**	29.877
min Q_{req}	3.529	0.265	6201.5	0.137	**0.143**
MOPSO+TOPSIS (Scenario S4, w2)	3.665	0.330	5867.6	0.09	5.210

S3, which balances active and reactive DG control, achieves the most significant reduction in power losses under both weightings: from the 24.97 MW of the modified network down to 1.038 MW under w_1 and 2.382 MW under w_2. In terms of the generation cost, S3 and S4 are the ones with the minimum value, indicating that the maximum injection of active power from DG sources produces the greatest economic benefits. Changing from weighting vector w_1 (which places greater emphasis on power losses and voltage deviation) to w_2 results in increased power losses across all scenarios, demonstrating how decision-maker preferences significantly impact the optimization results. The obtained results are consistent with the ones observed in (Candra *et al.,* 2024) on the same IEEE-30 network and PSO technique, reporting active power loss reductions when integrating renewable sources.

4.5. Single-objective versus multi-objective optimization

Table 3 shows for each individually minimized objective, the value of all five-objectives in the corresponding solution, compared to the compromise solution selected by the proposed methodology. Since the individual optimum of an objective corresponds to the extreme point of the Pareto front along that objective, the single-objective optima are obtained directly from the Pareto set already generated. Each single-objective solution is competitive in its own criterion but clearly degrades the others, and no single-objective solution is simultaneously acceptable across all five-objectives. The multi-objective + TOPSIS solution does not reach the individual optimum of any objective but remains balanced across all of them.

4.6. Reactive power market clearing via VCG

After the multi-objective optimization process and control vector selection with TOPSIS, we obtain the bus-level reactive power requirement of the DSO, Q_{req}. Let us consider one of the solutions for IEEE-30 network to evaluate payments for the reactive power auxiliary service by the DG. Let us consider that the reactive power requirement at bus 21 is 20.2 MVAr. For the market clearing stage, the DG unit connected at bus 21 is represented as an aggregated portfolio of ten smaller providers, made up of two conventional generators with a rated power of 7 and 6 MVA with relatively high reactive power costs, four solar plants with capacities between 3.5 and 5 MVA, and four wind plants with generators between 3.5 and 4.5 MVA.

Table 4 provides information on the type and quantity of DG plants connected to the common point of bus 21, where Q_{cap} is the maximum reactive power capacity of the generator in

Table 4
Generator characteristics, operating conditions, and economic settlements under the VCG auction mechanism at aggregated bus 21. Total reactive power demand: 20.2 MVAr.

	Generator Characteristics				Operation Conditions			Assignment Results				
	Type	Q_{cap} (MVAr)	S_n (MVA)	P_{max} (MW)	P_{actual} (MW)	Q_{avail} (MVAr)	Cost ($/MVAr)	Q_{assig} (MVAr)	Total Cost ($)	VCG Payment ($)	VCG Factor	Profit ($)
Gen 1	Conv	4.2	7	5	5	3.92	6.7	0	0	0	0	0
Gen 2	Conv	3.6	6	4	4	3.58	5.6	0	0	0	0	0
Gen 3	Solar	5.5	5	3.5	3.5	4.24	2.61	4.24	11.07	12.76	1.15	1.69
Gen 4	Solar	4.4	4	2.5	2.5	3.62	2.97	1.18	3.5	3.61	1.03	0.11
Gen 5	Solar	3.9	3.5	2	2	3.29	3.15	0	0	0	0	0
Gen 6	Solar	4.4	4	1.8	1.8	4.01	2.34	4.01	9.4	12.07	1.28	2.67
Gen 7	Wind	3.2	4	3	3	3.2	2.7	3.2	8.64	9.57	1.11	0.93
Gen 8	Wind	2.9	3.5	2.5	2.5	2.9	3.06	0	0	0	0	0
Gen 9	Wind	3.5	4.5	3.5	3.5	3.5	2.7	3.5	9.45	10.49	1.11	1.04
Gen 10	Wind	4.1	4.2	2.2	2.2	4.06	2.16	4.06	8.78	12.21	1.39	3.43

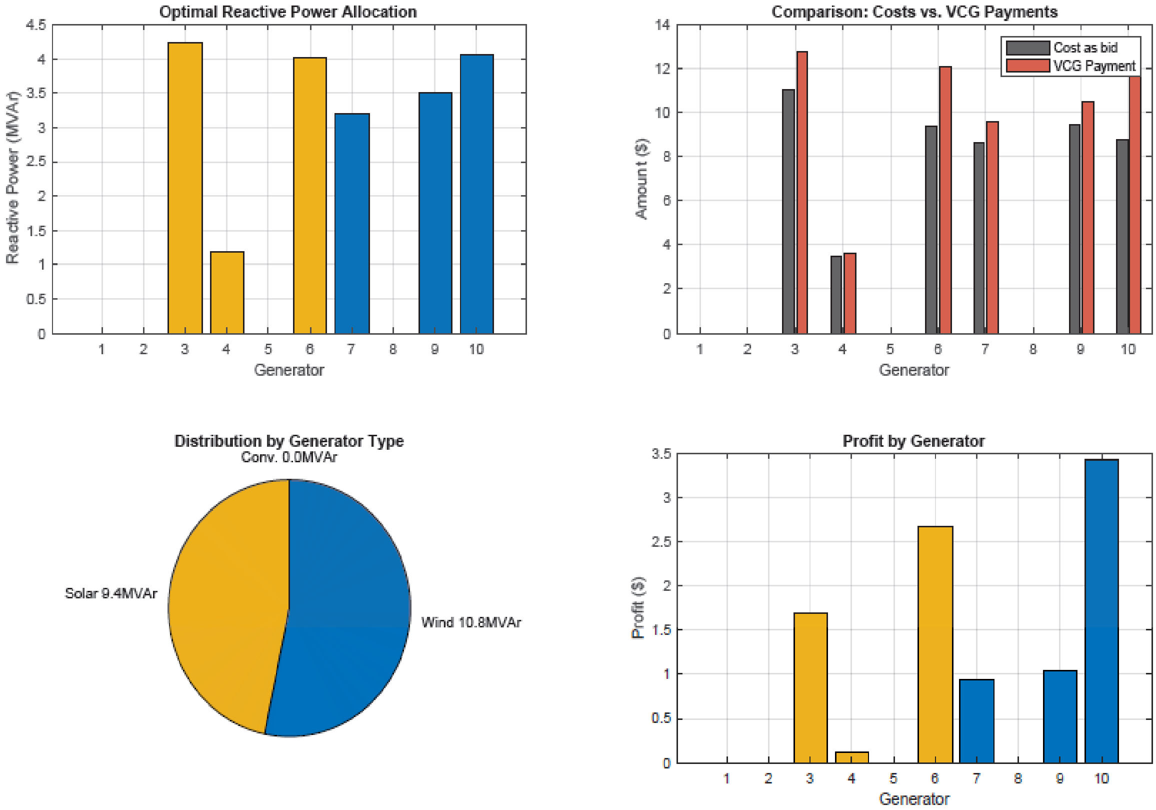

Fig. 6. Economic analysis of VCG mechanism: reactive power allocation, payment structures, and generator profit distribution

MVAr, *Cost* is the cost defined to provide reactive power to the DSO in $\$/MVAr$. P_{max} is the maximum active power it can supply and S_n is the nominal apparent power of the generating plant.
The available reactive capability of each unit is modeled according to its technology: conventional (synchronous) generators follow a circular capability curve $Q_{cap} = \sqrt{S^2 - P^2}$ with the operational restriction $Q_{cap} \leq 0.6\ S$. For solar plants which have power converters for connection to the grid, it is considered that reactive power can be provided even when there is no active generation. The reactive capability is calculated from the converter apparent-power limit considering a 10% oversizing factor. Finally, for wind generators, a semi-circular curve is followed with the same oversizing factor $Q_{cap} = \sqrt{(1.1S)^2 - P^2}$.

Table 4 and Figure 6 illustrate the provision of reactive power through the VCG auction at bus 21. At bus 21 there are several DG sources that can provide this auxiliary service, including conventional units, solar PV, and wind plants. The results show that conventional generators, despite having enough reactive capacity, were not selected due to their higher declared costs, while renewable units supplied 100% of the reactive demand (9.4 MVAr from solar, 10.8 MVAr from wind). This conclusion highlights the economic efficiency of the VCG mechanism, as it naturally prefers the lowest-cost suppliers while maintaining the overall benefit.

As a result of the auction, we obtain an optimal total cost of 50.84 $ for the supply of reactive power requested by the DSO, with total VCG payments of 60.71 $, which represents an additional cost for the VCG mechanism of 9.87 $ (19.41%). This additional cost is the main characteristic result of the VCG mechanism, which incentivizes honest bidding, ensuring that selected generators are compensated not only for their declared cost but also for their marginal contribution to the overall system. The extra VCG payment can be seen as the price of ensuring an incentive to participate in the service and to avoid market manipulation. This case demonstrates that the proposed mechanism achieves its objective of incentivizing the participation of DG in the reactive power market.

The implementation of reactive markets provides solar and wind plants with the opportunity to monetize their reactive capacity, even during periods of low active generation, while conventional units did not receive remuneration because their costs were not competitive. This emphasizes the idea that renewable DG sources can play a central role in reactive power support at the distribution level for modern future grids. This example illustrates how the standard VCG-based clearing mechanism can reduce incentives for strategic bidding and produce an efficient allocation under the assumed cost and availability conditions. Although this case study was conducted on a modified IEEE-30 bus system, the conclusions are general for the integration of DG into reactive markets, which supported by incentive mechanisms can reduce overall system costs, improve technical performance, and provide DG renewable sources with new income.

4.7. Sensitivity analysis

To address the robustness of the optimization and market results, a sensitivity analysis is conducted on the most influential input of the market clearing stage, the reactive power demand Q_{req} that the multi-objective optimization delivers to the auction. The demand is modified from 1 to 25 MVAr. The total reactive capability available at the aggregated bus is approximately 36

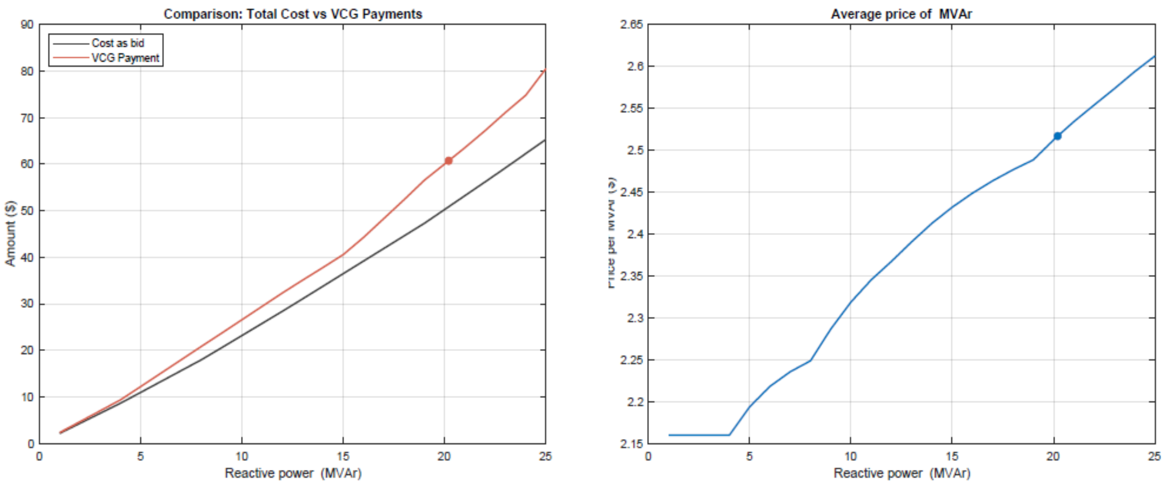

Fig. 7. Sensitivity analysis of the VCG mechanism, reactive power requirements vs payment structures.

MVAr and the largest single unit provides about 4 MVAr. Figure 7 summarizes the two main economic indicators.

The allocation is dominated by renewable units across the entire range: wind alone clears the demand for very small requirements ($Q_{req} \leq$ 4 MVAr), solar progressively joins from 5 MVAr, and above 13 MVAr both technologies share the supply, while conventional generators are not dispatched. VCG payments increase when the lowest cost renewable sources become exhausted and higher opportunity cost units become marginal. The average procurement cost is quite stable. As shown in Figure 7, it increases only from about 2.16 $/MVAr at 1 MVAr to 2.61 $/MVAr at 25 MVAr. Therefore, the average unit procurement price increases by approximately 20% while the requested quantity increases by a factor of 25. The mechanism therefore scales the cost of reactive procurement in an almost linear and highly predictable way, which is a key factor for DSOs that have to allocate reactive power under varying conditions.

From a market perspective, Potter *et al.* (2023) show that inverter-based resources can meet reactive demand with stable remuneration. Our VCG mechanism reaches an analogous conclusion and a stable average cost while additionally guaranteeing truthful cost disclosure. These results qualitatively confirm the trends reported by Xu *et al.* (2022) regarding the simultaneous improvement of losses, voltage profile and stability when exploiting the reactive capability of renewable DG.

5. Conclusions

This study has presented a comprehensive framework for electrical network optimization based on multi-objective metaheuristic algorithms, with the ultimate goal of establishing a reactive power market that incentivizes distributed generation units to provide reactive power support in high-penetration DG systems. The framework couples a five-objective MOPSO algorithm, balancing technical and economic objectives, with a TOPSIS based multi-criteria decision step that selects a single operating point from the Pareto front, and a VCG auction mechanism that allocates the reactive demand among several DG providers connected to the same bus.

Validation was performed on a modified IEEE-30 test system with 50 MW DG units at buses 19, 21 and 30 under stressed load conditions. The optimization of active and reactive power under scenario S3 reduced active power losses to 2.382 MW under the TOPSIS selection vector *w*.2, while simultaneously decreasing the mean voltage deviation and the cost of conventional generation. The hypervolume of the Pareto front improves from 0.485 in the baseline scenario to 0.823 under active-reactive control, showing that the addition of DG reactive capability not only improves the selected operating point but improves the entire objective space offered to the DSO.

From an economic perspective, the VCG auction allocated the reactive demand entirely to renewable units. The market clearing through the VCG auction mechanism provides an efficient allocation of reactive power, moving beyond traditional bilateral contracts or pay-as-bid auctions to ensure truthful cost disclosure from multiple small-scale DG providers. The fact that solar and wind plants displaced conventional generators in the auction reinforces the strategic role of renewable DG in the support of future networks, even during periods of low active generation, when the unused converter capacity can be redirected to reactive provision at minimal opportunity cost.

Future research will focus on extensions of the proposed framework. First, the incorporation of uncertainty for renewable generation, load demand patterns, and line parameters to ensure the robustness of the optimization model under imperfect information. Second, the validation in real networks with hundreds of DG units, where computational complexity and market resolution are critical. Third, the development of dynamic pricing mechanisms that incorporate variations in the value of reactive power, for example, during system contingencies or extreme weather events. Additionally, extend the framework to consider emerging technologies such as battery energy storage systems with full quadrant operation and electric vehicle aggregators as reactive power providers.

CRediT authorship contribution statement: All authors contributed equally to this work.

Funding: The authors received no specific funding for this work.

Conflict of interest: The authors declare no conflict of interest.

Data availability: Data will be made available on request.

References

Acosta, M. N., Gonzalez-Longatt, F., Andrade, M. A., Torres, J. L. R., & Chamorro, H. R. (2021). Assessment of daily cost of reactive power procurement by smart inverters. *Energies, 14*(16), Article 4834. https://doi.org/10.3390/en14164834

Anaya, K. L., & Pollitt, M. G. (2020). Reactive power procurement: A review of current trends. *Applied Energy, 270*, Article 114939. https://doi.org/10.1016/j.apenergy.2020.114939

Bamikole, O. J., Jibril, Y., Jimoh, B., Okorie, P. U., & Adamu, S. A. (2024). Optimal transmission voltage deviation based on fractional kinetic gas molecular optimization symbiotic organism search algorithm for network operational stability improvement. *Materials Today: Proceedings, 105*, 50–55. https://doi.org/10.1016/j.matpr.2023.07.005

Behzadian, M., Otaghsara, S. K., Yazdani, M., & Ignatius, J. (2012). A state-of-the-art survey of TOPSIS applications. *Expert Systems with Applications, 39*(17), 13051–13069. https://doi.org/10.1016/j.eswa.2012.05.056

Blaabjerg, F., Yang, Y., Yang, D., & Wang, X. (2017). Distributed power-generation systems and protection. *Proceedings of the IEEE, 105*(7), 1311–1331. https://doi.org/10.1109/JPROC.2017.2696878

Bozionek, J., Wolgast, T., & Nieße, A. (2022). Design and evaluation of a multi-level reactive power market. *Energy Informatics, 5*(1), Article 6. https://doi.org/10.21203/rs.3.rs-1389372/v1

Bukhsh, W. A., Grothey, A., McKinnon, K. I., & Trodden, P. A. (2013). Local solutions of the optimal power flow problem. *IEEE Transactions on Power Systems, 28*(4), 4780–4788. https://doi.org/10.1109/tpwrs.2013.2274577

Candra, O., Alghamdi, M. I., Hammid, A. T., Alvarez, J. R. N., Staroverova, O. V., Hussien Alawadi, A., Marhoon, H. A., & Shafieezadeh, M. M. (2024). Optimal distribution grid allocation of reactive power with a focus on the particle swarm optimization technique and voltage stability. *Scientific Reports, 14*(1), Article 10889. https://doi.org/10.1038/s41598-024-61412-9

Chen, S.-J., & Hwang, C.-L. (1992). Fuzzy multiple attribute decision making methods. In *Fuzzy multiple attribute decision making: Methods and applications* (pp. 289–486). Springer. https://doi.org/10.1007/978-3-642-46768-4_5

Coello, C. A. C., Pulido, G. T., & Lechuga, M. S. (2004). Handling multiple objectives with particle swarm optimization. *IEEE Transactions on Evolutionary Computation, 8*(3), 256–279. https://doi.org/10.1109/TEVC.2004.826067

Cramton, P. C., Shoham, Y., Steinberg, R., & Smith, V. L. (2006). *Combinatorial auctions* (Vol. 1). MIT Press. https://doi.org/10.7551/mitpress/9780262033428.003.0001

Eladl, A. A., Basha, M. I., & ElDesouky, A. A. (2022). Multi-objective-based reactive power planning and voltage stability enhancement using FACTS and capacitor banks. *Electrical Engineering, 104*(5), 3173–3196. https://doi.org/10.1007/s00202-022-01542-3

Gandhi, O. (2020). *Reactive power support using photovoltaic systems: Techno-economic analysis and implementation algorithms*. Springer Nature. https://doi.org/10.1007/978-3-030-61251-1_1

Halbhavi, S. B., Karki, S., & Kulkarni, S. G. (2012). Reactive power pricing framework problems and a proposal for a competitive market. *International Journal of Innovations in Engineering and Technology, 1*(2), 22–27.

Häselbarth, S., Winkels, O., & Strunz, K. (2023). Blockchain-based market procurement of reactive power. *IEEE Access, 11*, 36106–36119. https://doi.org/10.1109/access.2023.3263669

Hasanvand, S., Sobhani, H., & Khooban, M.-H. (2025). Distribution network clustering for reactive power planning and distributed voltage control. *IET Generation, Transmission & Distribution, 19*(1), Article e70002. https://doi.org/10.1049/gtd2.70002

Huang, Y.-S., & Li, W.-H. (2012). A study on aggregation of TOPSIS ideal solutions for group decision-making. *Group Decision and Negotiation, 21*, 461–473. https://doi.org/10.1007/s10726-010-9218-2

Iweh, C. D., Gyamfi, S., Tanyi, E., & Effah-Donyina, E. (2021). Distributed generation and renewable energy integration into the grid: Prerequisites, push factors, practical options, issues and merits. *Energies, 14*(17), Article 5375. https://doi.org/10.3390/en14175375

Javed, A. H., Nguyen, P. H., Morren, J., & Slootweg, J. G. H. (2023). Using smart PV inverters for reactive power management in distribution grids. In *2023 IEEE PowerTech Belgrade*. IEEE.

Ji, Y., Chen, X., He, P., Liu, X., Wu, X., & Zhao, C. (2023). A novel voltage/var sensitivity calculation method to partition the distribution network containing renewable energy. *Recent Advances in Electrical & Electronic Engineering, 16*(4), 380–394. https://doi.org/10.2174/2352096516666221130150549

Li, Z., & Xiong, J. (2024). Reactive power optimization in distribution networks of new power systems based on multi-objective particle swarm optimization. *Energies, 17*(10), Article 2316. https://doi.org/10.3390/en17102316

Liu, X., Zhang, P., Fang, H., & Zhou, Y. (2021). Multi-objective reactive power optimization based on improved particle swarm optimization with ε-greedy strategy and Pareto archive algorithm. *IEEE Access, 9*, 65650–65659. https://doi.org/10.1109/access.2021.3075777

Liu, Y., Chen, M., Fan, Y., Ying, L., Cui, X., & Zou, X. (2024). Design of a stochastic electricity market mechanism with a high proportion of renewable energy. *Energies, 17*(12), Article 3044. https://doi.org/10.3390/en17123044

Malik, S., Thakur, S., Duffy, M., & Breslin, J. G. (2023). Comparative double auction approach for peer-to-peer energy trading on multiple microgrids. *Smart Grids and Sustainable Energy, 8*(4), Article 21. https://doi.org/10.1007/s40866-023-00178-x

Miraftabzadeh, S. M., Colombo, C. G., Longo, M., & Foiadelli, F. (2023). K-means and alternative clustering methods in modern power systems. *IEEE Access, 11*, 119596–119633. https://doi.org/10.1109/access.2023.3327640

Mohammed, A., Sakr, E. K., Abo-Adma, M., & Elazab, R. (2024). A comprehensive review of advancements and challenges in reactive power planning for microgrids. *Energy Informatics, 7*(1), Article 63. https://doi.org/10.1186/s42162-024-00341-3

Molzahn, D. K., Dörfler, F., Sandberg, H., Low, S. H., Chakrabarti, S., Baldick, R., & Lavaei, J. (2017). A survey of distributed optimization and control algorithms for electric power systems. *IEEE Transactions on Smart Grid, 8*(6), 2941–2962. https://doi.org/10.1109/TSG.2017.2720471

Mugemanyi, S., Qu, Z., Rugema, F. X., Dong, Y., Bananeza, C., & Wang, L. (2020). Optimal reactive power dispatch using chaotic bat algorithm. *IEEE Access, 8*, 65830–65867. https://doi.org/10.1109/ACCESS.2020.2982988

Musirin, I., & Rahman, T. K. A. (2002). Novel fast voltage stability index (FVSI) for voltage stability analysis in power transmission system. In *Student Conference on Research and Development* (pp. 265–268). IEEE. https://doi.org/10.1109/scored.2002.1033108

Nkalo, U. K., Inya, O. O., Obi, P. I., Bola, A. U., & Ewean, D. I. (2024). A modified multi-objective particle swarm optimization (M-MOPSO) for optimal sizing of a solar–wind–battery hybrid renewable energy system. *Solar Compass, 12*, Article 100082. https://doi.org/10.1016/j.solcom.2024.100082

Potter, A., Haider, R., Ferro, G., Robba, M., & Annaswamy, A. M. (2023). A reactive power market for the future grid. *Advances in Applied Energy, 9*, Article 100114. https://doi.org/10.1016/j.adapen.2022.100114

Prioste, F. B. (2021). Optimal power flow using genetic algorithm. In *Anais do 15 Congresso Brasileiro de Inteligência Computacional* (pp. 1–6). https://doi.org/10.21528/cbic2021-144

Qiu, D., Baig, A. M., Wang, Y., Wang, L., Jiang, C., & Strbac, G. (2024). Market design for ancillary service provisions of inertia and frequency response via virtual power plants: A non-convex bi-level optimisation approach. *Applied Energy, 361*, Article 122929. https://doi.org/10.1016/j.apenergy.2024.122929

Ruan, H., Gao, H., Liu, Y., Wang, L., & Liu, J. (2020). Distributed voltage control in active distribution network considering renewable energy: A novel network partitioning method. *IEEE Transactions on Power Systems, 35*(6), 4220–4231. https://doi.org/10.1109/tpwrs.2020.3000984

Sachan, S., Mishra, S., Øyvang, T., & Bordin, C. (2025). Minimizing active power losses and voltage deviations for reactive power planning considering bus vulnerability. *Next Research*, Article 100633. https://doi.org/10.1016/j.nexres.2025.100633

Safari, A., Salyani, P., & Hajiloo, M. (2020). Reactive power pricing in power markets: A comprehensive review. *International Journal of Ambient Energy, 41*(13), 1548–1558. https://doi.org/10.1080/01430750.2018.1517675

Siahroodi, H. J., Mojallali, H., & Mohtavipour, S. S. (2022). A new stochastic multi-objective framework for the reactive power market considering plug-in electric vehicles using a novel metaheuristic approach. *Neural Computing and Applications, 34*(14), 11937–11975. https://doi.org/10.1007/s00521-022-07081-z

Singh, K., Padhy, N. P., & Sharma, J. (2011). Transmission expansion planning including reactive power procurement in deregulated environment. *Electric Power Components and Systems, 39*(13), 1403–1423. https://doi.org/10.1080/15325008.2011.584110

Tesfatsion, L. (2020). *A new swing-contract design for wholesale power markets.* John Wiley & Sons. https://doi.org/10.1002/9781119670155

Wolgast, T., Ferenz, S., & Nieße, A. (2022). Reactive power markets: A review. *IEEE Access, 10*, 28397–28410. https://doi.org/10.1109/ACCESS.2022.3141235

Wood, A. J., Wollenberg, B. F., & Sheblé, G. B. (2013). *Power generation, operation, and control.* John Wiley & Sons.

Wu, J., Li, N., He, L., Yin, B., Guo, J., & Liu, Y. (2010). Research on multi-objective reactive power optimization based on modified particle swarm optimization algorithm. In *2010 Chinese Control and Decision Conference* (pp. 477–480). IEEE. https://doi.org/10.1109/ccdc.2010.5499012

Xu, B., Zhang, G., Li, K., Li, B., Chi, H., Yao, Y., & Fan, Z. (2022). Reactive power optimization of a distribution network with high-penetration of wind and solar renewable energy and electric vehicles. *Protection and Control of Modern Power Systems, 7*(1), Article 51. https://doi.org/10.1186/s41601-022-00271-w

Zhang, J., Tang, Q., Li, P., Deng, D., & Chen, Y. (2016). A modified MOEA/D approach to the solution of multi-objective optimal power flow problem. *Applied Soft Computing, 47*, 494–514. https://doi.org/10.1016/j.asoc.2016.06.022

Zhang, X., Chen, Y., Wang, Y., Ding, R., Zheng, Y., Wang, Y., Zha, X., & Cheng, X. (2020). Reactive voltage partitioning method for the power grid with comprehensive consideration of wind power fluctuation and uncertainty. *IEEE Access, 8*, 124514–124525. https://doi.org/10.1109/access.2020.3004484

Zimmerman, R. D., Murillo-Sánchez, C. E., & Thomas, R. J. (2010). MATPOWER: Steady-state operations, planning, and analysis tools for power systems research and education. *IEEE Transactions on Power Systems, 26*(1), 12–19. https://doi.org/10.1109/TPWRS.2010.2051168